

Sunspot waves and flare energy release

R. Sych¹, M. Karlický², A. Altyntsev¹, J. Dudík³ and L. Kashapova¹

¹Institute of Solar-Terrestrial SB RAS, Lermontov st. 126a, 6640333 Irkutsk, Russia

²Astronomical Institute of the Academy of Sciences of the Czech Republic, 25165 Ondřejov, Czech Republic

³RS Newton International Fellow, DAMTP, CMS, University of Cambridge, Wilberforce Road, Cambridge CB3 0WA, United Kingdom

Received / Accepted

ABSTRACT

Context. We address a possibility of the flare process initiation and further maintenance of its energy release due to a transformation of sunspot longitudinal waves into transverse magnetic loop oscillations with initiation of reconnection. This leads to heating maintaining after the energy release peak and formation of a flat stage on the X-ray profile.

Aims. We present a study of correlation between sunspot 3-min slow magnetoacoustic wave dynamics and the flare emergence process. Propagating waves in the magnetic loop, whose one foot is anchored in umbra, represent the disturbing agent responsible for energy release initiation.

Methods. We applied the time-distance plots and pixel wavelet filtration (PWF) methods to obtain spatio-temporal distribution of wave power variations in SDO/AIA data. To find magnetic waveguides, we used magnetic field extrapolation of SDO/HMI magnetograms. The propagation velocity of wave fronts was measured from their spatial locations at specific times.

Results. In correlation curves of the 17 GHz (NoRH) radio emission we found a monotonous energy amplification of 3-min waves in the sunspot umbra before the 2012 June 7 flare. This dynamics agrees with an increase in the wave-train length in coronal loops (SDO/AIA, 171 Å) reaching the maximum ~ 30 minutes prior to the flare onset. A peculiarity of this flare time profile in soft X-rays (RHESSI, 3-25 keV) is maintaining the constant level of the flare emission for ~ 10 minutes after the short impulse phase, which indicates at the energy release continuation. Throughout this time, we found 30-sec period transverse oscillations of the flare loop in the radio-frequency range (NoRH, 17 GHz). This periodicity is apparently related to the transformation of propagating longitudinal 3-min waves from the sunspot into the loop transverse oscillations. The magnetic field extrapolation based on SDO/HMI magnetograms showed the existence of the magnetic waveguide (loop) connecting the sunspot with the energy release region. A flare loop heating can be caused by the interaction (reconnections) of this transversally oscillating waveguide with the underlying twisted loops.

Conclusions. We analyzed the sunspot 3-min wave dynamics and found a correlation between the oscillation energy amplification and the flare triggering in the region connected to the sunspot through the magnetic waveguide. Due to the loop heating, the wave velocity (sound velocity) increased with their penetration into the energy release site. The heating is shown to be able to proceed after the flare main peak owing to the energy pumping in the form of longitudinal waves from the sunspot which are then transformed into the flare loop transverse oscillations, and thus initiating an additional reconnection in the flare region.

Key words. Sun: flares – Sun: oscillations – Sun: X-rays

1. Introduction

The first ideas of solar flare initialization were described by Norman & Smith (1978). They argued that flare process cannot start in all the flare volume at one instant. The flare onset was proposed to be localized in a small part of an active region, and then the energy release extends as dissipation spreading process throughout the flare volume. Two types of agents that may lead to such a dissipation process were addressed: a) electron beams, and) shock waves. These agents may trigger flares at large distances from their initial locations, causing sympathetic (simultaneous) flares or leading to a sequential flare energy release in one active region (Liu et al. 2009; Zuccarello et al. 2009). These triggering processes were numerically studied by Karlický & Jung-

wirth (1989) and Odstrčil & Karlický (1997). In the first paper, Karlický & Jungwirth (1989) assumed that electron beams, penetrating into the current sheet in the magnetic reconnection region, generate Langmuir waves. Then, using the particle-in-cell model, the authors studied effects of these electrostatic waves on the plasma system. Sufficiently strong Langmuir waves were found to be able to generate ion-sound waves through the three-wave decay process (Bárta & Karlický 2000). These ion-sound waves increase electrical resistivity in the current sheet system, which results in the energy dissipation process onset. Thereby, electron beams were concluded to be able to cause magnetic reconnection. On the other hand, Odstrčil & Karlický (1997) studied the mechanism for the flare trigger by shock waves. They used a 2-D magnetohydrodynamic model with the MHD shock wave propagating toward the current sheet. A

Send offprint requests to: R. Sych, e-mail: sych@iszf.irk.ru

portion of the shock wave passed through the sheet, the rest was reflected. Nothing occurred at the very beginning of the wave-current sheet interaction. However, after some time specific plasma flows around the current sheet were formed, which led to the start of magnetic reconnection. This shows that for reconnection to be triggered, not only the enhanced electrical resistivity is important, but also plasma flows. Also, one of the reconnection causes may be spatio-temporal dynamics of magnetic loops. Recently, using the SDO/AIA data, Dudík et al. (2014) presented a motion of magnetic loops with the slipping reconnection before the impulse phase of the 2012 June 12 eruptive flare. At this flare phase, the footpoints exhibited significant motions at speeds of about several tens of kilometers per second along expanding flare ribbons. Further, after the energy release peak, the loop motions and reconnections proceeded. At this time, a weak coronal mass ejection visible in the SDO/AIA 131 Å wavelength was also observed. Besides the above triggers of reconnection (beams and shocks), there is another agent, namely, magneto-hydrodynamic waves. In the paper by Nakariakov et al. (2006), these waves near the X-point were shown to be strongly amplified and thus triggering reconnection. Further, in Sych et al. (2009), by using observational data, it was shown that, ~ 20 min prior to the flare onset, a power maximum of slow magnetoacoustic waves that propagate from sunspots into the flare region is observed. It was proposed that these waves, propagating along magnetic loop channels, penetrate into the current sheet region and initiate the flare process.

The goal of this paper is to study the temporal and spatial dynamics of 3-min sunspot oscillations in active region NOAA 11494 on 2012 June 7, and their relation to the start and evolution of a small C-class flare originated next to the sunspot. This flare was thoroughly studied by Kotřč et al. (2013). We investigated the dynamics of the sources of umbra oscillations and of the formed flare loop in the radio, ultraviolet and X-ray ranges. To detect wave processes along the selected directions, we used the time-distance plot method. To calculate narrow-band images of the sources in the selected spectral range, we applied the pixel wavelet filtration (PWF-analysis) (Sych & Nakariakov 2008), and also the fast Fourier transform (FFT-analysis). Magnetic field extrapolation was performed using the Fourier Transform method of Alissandrakis (1981) and Gary (1989). The paper is organized as follows: In Section 1 we provide an introduction into the subject. In Section 2 observational data are presented. In Section 3 the data analysis in the radio and ultraviolet ranges is described and in Section 4 a scenario of the flare process evolution is presented. Section 5 provides the results and conclusions.

2. Observations

The 2012 June 7 flare occurred in the active region NOAA 11494 at 05:00-06:10 UT with the maximum near 05:56 UT. The flare importance was C1.5. The active region was located near the central meridian (S18, W20) and involved a large symmetric sunspot. We used cubes of images in UV obtained with the Atmospheric Imaging Assembly instrument (AIA, Title et al. 2006, Lemen et al. 2012) onboard the Solar Dynamics Observatory (SDO/AIA, Schwer et al. 2002) in the 171 Å (Fe IX) and 94 Å (Fe XVI) bands. The temporal resolution was 12 seconds and the spatial resolution between pixels was 0.6 arcsec. The observation dura-

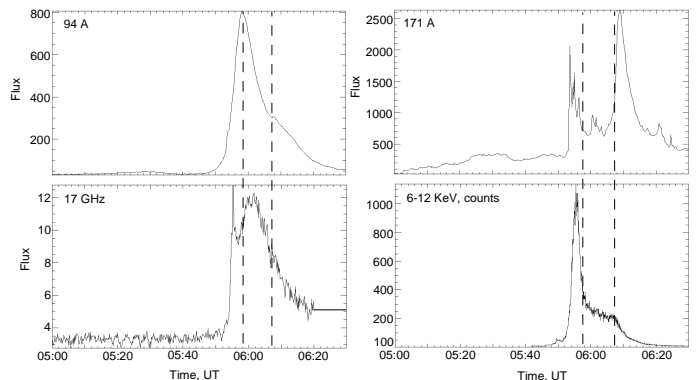


Fig. 1. The light curves of the 2012 June 7 flare in EUV channels (SDO/AIA, 94 Å and 171 Å), radio (NoRH, 17 GHz) and X-ray (RHESSI, 6-12 keV). The flat stage is shown by vertical dashed lines 05:58 - 06:08 UT.

tion was 1.5 hours (05:00-06:30 UT), which allowed us to study the sunspot oscillations within 0.5 - 30 min periods, and to trace the evolution of the flare process in the active region. We also used the Nobeyama Radio Heliograph data (17 GHz, images, correlation curves) in the radio range, and the Callisto BLEN (200-800 MHz) and Ondřejov (800-2000 MHz) radiospectra. In the X-ray range, the RHESSI data (6-12 keV) were used. We investigated the site on the Sun encompassing active region NOAA 11494, 120 x 120 arcsec in size, with the evolved symmetric sunspot in the center. The umbra size was ~ 12 arcsec, the penumbra being ~ 10 arcsec. To obtain the images, we used the SDO/AIA http://www.lmsal.com/get_aia_data/ resource that allows us to obtain calibrated images of the Sun (Lev1) for different wavelengths and in the given time interval. To convert the data (to center and intercalibrate for different wavelengths), the SolarSoft package was used. The source selection was performed manually, by assigning the active region center coordinates and the site dimensionality. The given object differential rotation within the observation day was removed by introducing an integer shift using the algorithm implemented at the website.

3. Analysis

3.1. Flare profiles

Fig. 1 presents the flare flux profiles obtained in the radio (NoRH, 17 GHz, intensity), in ultraviolet (SDO/AIA 171 Å and 94 Å), and in the soft X-ray (RHESSI) ranges. One can see that the profiles have three peaks at different instants. The first peak at $\sim 05:55$ UT is observed in most the wavelengths with different intensity. The second peak near 06:00 UT has the maximum at the chromospheric level (radio, 17 GHz) diminishing toward the corona (171 Å). The peak in the 94 Å channel shows the existence of high-temperature processes. There is also the third peak at $\sim 06:09$ UT visible in the 171 Å coronal line only. This evidences of a spatial-height dynamics of the flare energy release sources.

Note the formation of a flat interval on the X-ray profile at 05:58-06:06 UT. The flare loops are spatially near the sunspot. Some loops are anchored in the umbra where a continuous propagation of slow magnetoacoustic waves

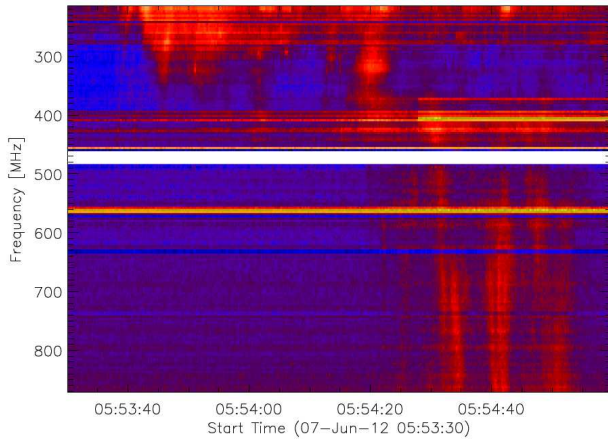


Fig. 2. The Callisto BLEN radio spectrum observed during the 2012 June 7 flare.

within the 3-min range of periods is observed. One may assume, that the wave processes are related to the flare processes, and to the flat interval in X-rays. To study this assumption, we investigated spatio-temporal parameters of the oscillation sources in the sunspot and flare loops.

3.2. Radio data analysis

3.2.1. Dynamic spectra analysis

The Callisto BLEN (200–800 MHz) (Fig. 2) and Ondřejov (800–2000 MHz) radio spectra show that the radio flare started with the type III bursts at 05:53:40–05:54:24 UT in the 200–400 MHz range. It shows that these processes started at about of 400 MHz, i.e. at the plasma density $n_e = 1.98 \times 10^9 \text{ cm}^{-3}$ (fundamental emission) or $n_e = 4.98 \times 10^8 \text{ cm}^{-3}$ (harmonic emission). Then at 05:54:24–05:55 UT broadband (200–2000 MHz) type III bursts together with the reverse drift bursts in the 800–1300 MHz appeared. These bursts, which designated the impulsive phase of the flare, were followed by a noise storm in the 200–300 MHz range.

3.2.2. Dynamics of oscillations before the flare

The radio-emission correlation curves in the NoRH 17 GHz frequency showed significant oscillations in the range near the 3-min period before the flare. The signals from small-angular size sources (<20 arcsec) in the form of spots or flare cores (Shibasaki 2001) are well-known to be the main contribution to the correlation curve variations. At the observations, there was only one strongly polarized radio source on the solar disk associated with the sunspot in the studied NOAA 11494 active region. One may assume that the observed oscillations are related to this source. We processed the flare correlation curve signal within 04:00–06:30 UT through wavelet transformation. The obtained wavelet spectrum within the 2–4 min periods showed a series of 3-min oscillation trains, which the power was increasing before the flare (Fig. 3). The train duration was ~ 12 –20 minutes, which agrees well with the previously published results (Sych et al. 2009, Abramov-Maksimov et al. 2011). We can see that the oscillations grew linearly and started two hours prior to the flare onset. The oscillation power peak

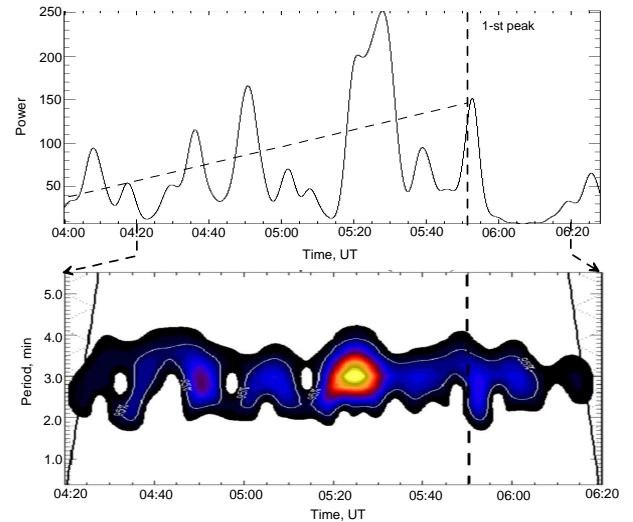


Fig. 3. Top panel: The power variations at the NoRH, 17 GHz correlation curve in the polarization channel centered at 5.6 mHz frequency. The dotted line shows the trend of increasing 3-min oscillations before the radio burst. The burst maximum (1-st peak) is shown by vertical line. Bottom panel: Wavelet power spectrum of oscillations

was observed at 05:30 UT, ~ 20 –30 minutes before the main flare maximum. Throughout each train, the instantaneous period of oscillations drifted within 2–4 minutes. This indicates (Sych et al. 2012) that waves propagated in spatially distributed magnetic loops with different cut-off frequencies determined by physical (plasma temperature) and geometrical (inclination angles) parameters of these waveguides. As the flare onset approaches, one observes a decrease in the range of oscillation periods and drift velocities. This testifies a formation of a single rope of magnetic waveguides with nearly the same parameters (magnetic channel). One may assume that the oscillation energy boost and the channel formation along which waves propagate are interdependent processes determining the flare emergence. In this context, waves appear like the flare energy release trigger (Sych et al. 2009).

3.2.3. Spatial evolution of the flare radio source

To test this last statement and to obtain the radio source spatial pattern prior to and during the flare, we synthesized the radio sources (NoRH, 17 GHz) over 05:00–06:20 UT with the 10-sec temporal resolution. Fig. 4 shows individual images in the intensity channel (black continuous contours) and circular polarization (white color, dotted contours), superposed on coronal images in ultraviolet (SDO/AIA, 171 Å). The images were obtained for instants prior to the flare (05:53:20 UT) and for the energy release peak times (05:54:50 UT, 05:58:50 UT, and 06:10:20 UT). One can see (Fig. 4) that there exists a loop-like source in the intensity channel prior to the flare at 05:53:20 UT. One of the footpoints is anchored in the umbra. White dotted contours indicate the strongly polarized sunspot. Radio loop contours approximately coincide with the coronal loop visible in the UV 171 Å channel. At time of the 1st flare maximum at 05:54:50 UT, a displacement of the loop top (in projection) and the formation of a new flare loop occur.

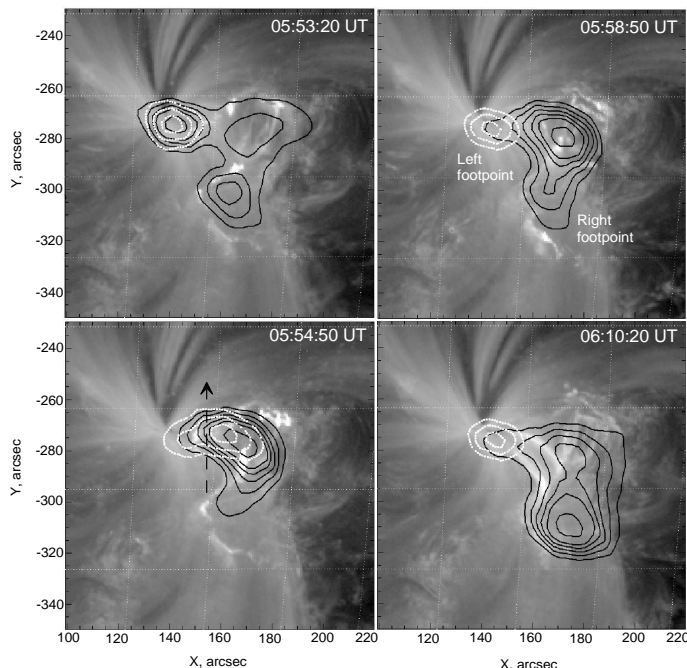


Fig. 4. Time evolution of the microwave burst (NoRH, 17 GHz) observed during the 2012 June 7 flare. The black solid lines signify intensity, white dotted line is polarization. The background is a 171 Å image. The arrow shows the path of scans for the time-distance plot.

From the sunspot, along the loop left foot, a new polarized source (generated by the gyro-synchrotron emission) starts to form, which indicates heating a part of the loop anchored in the sunspot. The heating is related to the 3-min wave trains and with their growth (Fig. 3). At 05:58:50 UT (2nd flare maximum) and 06:10:20 UT (3rd flare maximum), the radio loop flattens (Fig. 4) coinciding with the new coronal loops originated in ultraviolet emission at 171 Å. The waves from the sunspot propagate along the new loop, and may lead to the generation of loop transverse oscillations (Zaitsev & Stepanov 2009).

3.2.4. Radio loop oscillations

To study the sunspot wave dynamics and the flare loop oscillations during the flare, we used the coordinate-time diagram by radio images (NoRH, 17 GHz) in the polarization channel. The arrow in Fig. 4 shows the scanning direction at 05:54:50 UT. To obtain spectral components, we used global wavelet spectra. One can see (Fig. 5) that, during the flare, there emerged well-defined transverse loop oscillations with a 35-sec mean period noted earlier in a number of papers (e.g. Kupriyanova et al. 2013). Prior to the flare, there was no periodicity observed out of the sunspot. Then the V-shaped forms were generated as a result of recurrent motions (Fig. 5, left panel). The maximal spatial shift of the oscillating loop was observed during the flare peak at 05:54:30–05:56:20 UT with its gradual damping during the flat stage on the X-ray curve (Fig. 1). The spatial shifts in sunspot and at the footpoint are minimal. This periodic transverse component of the oscillations was found in the whole loop; changing from minimal values (~ 30 sec) in the sunspot and in the loop top to maximal (~ 36 sec) between

them. The oscillation power grows toward the middle of the loop foot. Along with these periods, there exist peak periods within the ~ 56 –70 sec range in the wavelet spectrum. Their behavior is similar to a higher-frequency component. Also, there are well-known 3-min sunspot oscillations with ~ 185 –223 sec periods.

One may assume that the revealed periodicity along the loop is a response to 3-min sunspot oscillations. The increase in longitudinal wave oscillations prior to and during the flare led to their transformation into transverse oscillations. One can see well in the images (Fig. 5, right panel) that the radio loop central part transversally oscillates. The sunspot central part remains spatially unchanged and the loop top oscillates only slightly.

3.3. UV data analysis

The above radio investigations at the transition region level show that there exists an energy boost in propagating waves before the flare onset in a sunspot. There occurs a formation of a uniform waveguide in the form of a new loop-like radio source along which the waves start to permeate into the flare region. We assume that this process will also be observed at higher levels, in the corona. To study these processes, we analyzed the SDO/AIA ultraviolet images obtained at the 171 Å and 94 Å wavelengths. Accounting for the significant difference between the NoRH angular resolution (~ 10 arcsec) and SDO (~ 0.6 arcsec), one may expect a more detailed picture of the flare spatial evolution.

3.3.1. Spatial evolution of flare loops

First bright dots within the flare were recorded at 05:49:44 UT. Fig. 6 shows the evolution of flare loops prior to and during the flare (05:51:36, 05:54:24, and 06:10:36 UT). The 171 Å flare started with a brightening of the loop structure whose footpoints were anchored in its ribbons. Simultaneously a distance of these ribbons increased. These changes occurred at the first maximum on the flare profiles (Fig. 1). There also appears a new loop structure visible in the radio (Fig. 4) and in the ultraviolet emissions (Fig. 6). One of the loop footpoints is anchored in the sunspot. Further, plasma heating led to the second peak near $\sim 06:00$ UT with the loop brightness maximum in the 94 Å hot coronal line (Fig. 7). Its onset coincides with the start of the 05:58–06:06 UT flat stage on the soft X-ray 6–12 keV (RHESSI) curve. The flare loop visibility maximum in the 171 Å cold coronal line falls at 06:10 UT (Fig. 6), and is related to the formation of the third brightness peak on the flare profile.

Analyzing the loops, we found that there is a magnetic channel that connects the sunspot to the flare energy release site. At the beginning of the flare, the loops in the 94 Å high-temperature channel were located below this channel and had a strong twist. The flare ribbons of these twisted loops were evolving fast over the flare impulsive phase, 05:52:30 through 05:55:00 UT, in association with meter and decimeter bursts (Fig. 2). The expansion of the flare loops was accompanied by the slipping reconnections as described by Aulanier et al. (2006, 2012) and Dudík et al. (2014).

Using the magnetic field extrapolation into the corona, made from an SDO/HMI magnetogram obtained at 06:00 UT, we searched for magnetic channel (waveguide). Al-

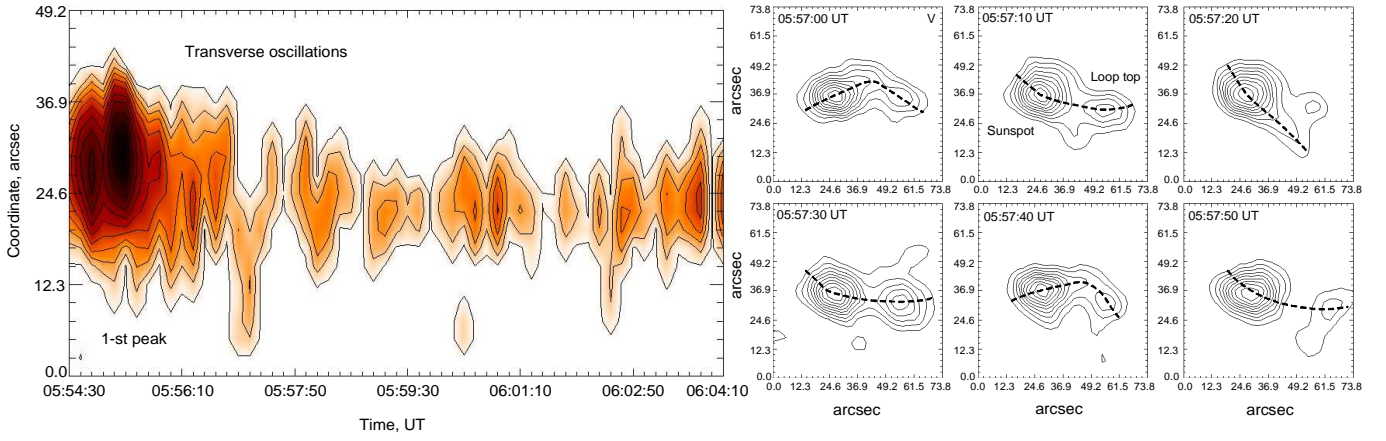


Fig. 5. Induced transverse oscillations of flare loop in 17 GHz (NoRH) polarization channel. Left panel: The time distance plots of oscillations. Right panel: Images of the radio sources during transverse oscillations at 05:57:00–05:57:50 UT.

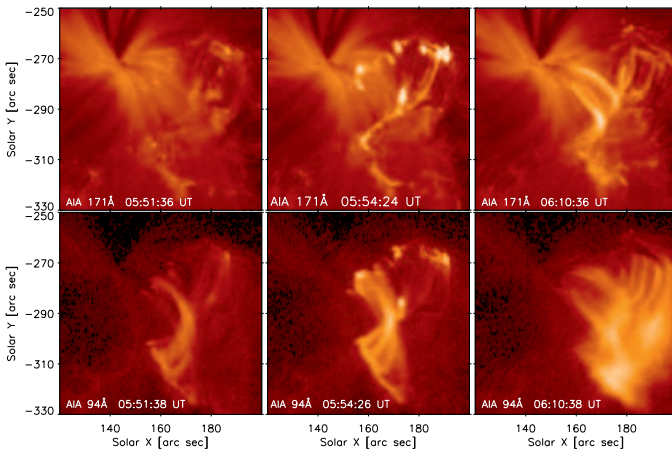


Fig. 6. Flare loop evolution in the 171 Å and 94 Å lines during the 2012 June 7 flare at three instants: 05:51:36 (:38), 05:54:24 (:26), and 06:10:36 (:38) UT.

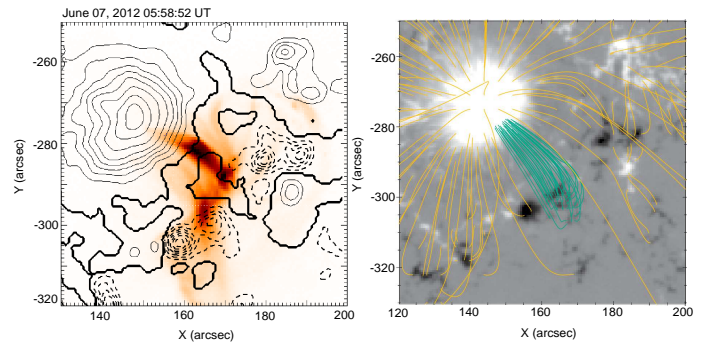


Fig. 7. Left panel: Image of flare loops in hot temperature channel (94 Å) at 05:58:52 UT. Contours show the magnetic field at the photosphere (SDO/HMI magnetogram). Right panel: Extrapolated magnetic field lines. The green lines mean the magnetic channel (waveguide) for 3-min oscillations.

though we consider only potential extrapolation, we found this magnetic channel, see Fig. 7. This magnetic channel persisted at the same location throughout the entire flare. Further, after the main phase at 06:10:36 UT, a 94 Å flare loop was formed that coincided with the magnetic channel, compare the left and right parts of Fig. 7. Its new orientation shows that the twisted loops located here prior to the flare onset changed their orientation, and became oriented as the magnetic channel in potential approximation. This means that electric currents in these loops decreased during the flare, i.e. their energy was released. Both the magnetic field lines of the channel and 94 Å hot loop are anchored in the sunspot with the southern polarity, their other foot-point is associated with the northern polarity (Fig. 7).

3.3.2. One-dimensional dynamics of waves in coronal loops

To study the dynamics of waves propagating from the sunspot along the coronal loops into the flare region, we used time-distance plots for the 171 Å and 94 Å waves (Fig. 8). The first 171 Å UV line images correspond to the cold coronal plasma with the temperature of about 1 MK, the other correspond to hot plasma (~ 6.3 MK).

The scanning direction of brightness temporal variations was selected along the wave-guiding loop starting from the sunspot.

One can see (Fig. 8, left panel) that ~ 3 -min waves propagate continuously in the umbra region. The horizontal dashed line shows the umbra boundary. About 30 minutes prior to the flare beginning, there occurs an increase in the train length and in the oscillation power. This moment coincided with the increase in the oscillations at the transition region level (Fig. 3). This indicates that the same wave process occurs both in the lower and in the upper umbra atmosphere. The train extension led to their over-running the umbra boundary. A new magnetic loop (Fig. 6) along which waves reach the flare region starts to form. Both temporally and spatially, the formation of the coronal loop coincides with the new loop in the radio range (Fig. 4). One observes an increase in the wave train inclination (see a series of steep features under the umbra border in Fig. 8, left part). These changes are related to the loop heating at 06:00 UT well seen in the 94 Å high-temperature channel (Fig. 8, right panel) and through an increase in the wave propagation velocity outside the umbra. We measured the wave train inclinations along the loop near the umbra center and at ~ 10 arcsec from its boundary. The calculated wave velocity is $V_1 = 36.2$ km s $^{-1}$ and $V_2 = 84.6$ km s $^{-1}$, re-

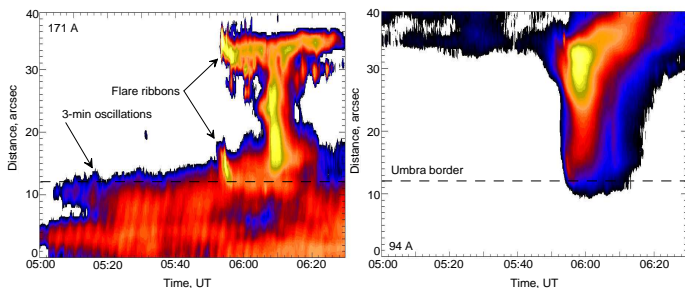


Fig. 8. Time-distance plots of flare region in 171 Å and 94 Å (SDO/AIA).

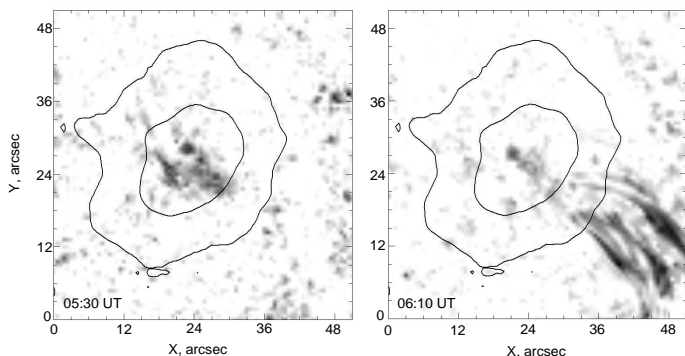


Fig. 9. Narrowband images of 3-min oscillations sources before (left panel) and maximum of the flare (right panel) at 171 Å.

spectively. The velocity values indicate that these waves are slow magnetosonic waves whose velocity is near the speed of sound. The kinetic temperature calculated for these two spatial regions is thus $T_1 = 47700$ K and $T_2 = 260000$ K, respectively.

3.3.3. Spatial structure of magnetic waveguides

To obtain a fine spatial structure of the flare loop in 171 Å, we used the pixel wavelet filtration (PWF analysis) (Sych & Nakariakov 2008). Narrowband images of magnetic waveguides within the 1.5-3.5 min band were built. One can see (Fig. 9, left panel), that prior to the flare, at 05:30 UT, the 3-min wave trains had a shape of an arrow with the footpoints in the umbra directed toward the future flare. At this time, all the oscillations occurred within the umbra boundary. Further, an extension of the wave train and their displacement into the penumbra is observed. There emerged a rope of thin loops at 06:10 UT along which waves propagate into the flare region. Fig. 8 shows this rope like a bright extended feature connecting the flare ribbons. One of the rope footpoints is anchored in the umbra, the other has several endings. The spatial location of the rope correlates well with the flare loop in the radio range (Fig. 4) and with the magnetic channel (Fig. 7), and corroborates the idea that just before the flare the wave trains started to be directed to the flare site. It also agrees to the range decrease of oscillation periods found in the analysis of the correlation curves (Fig. 3).

4. Flare scenario

The observational data in the radio (NoRH) and ultraviolet (SDO/AIA) ranges show an explicit association between the oscillatory processes occurring in the sunspot and the flare emergence in the adjacent region. There exists a linear increase in the power of 3-min oscillations in the radio source associated with the sunspot prior to the flare onset. This increase may be associated with a temporary increase in generating broadband impulses in the subphotospheric layers due to convection motions, local reconnections, etc. In the paper by Sych et al. (2009), this increase was interpreted like a wave trigger of the flare. The observed decrease in the range of oscillation periods and drifts allows us to conclude that there formed a special magnetic waveguide (channel) composed from many sub-channels which have nearly the same physical and geometrical properties. One may assume that this channel connects the sunspot region to the flare region. The flare temporal dynamics in the radio range showed a formation of a new flare loop (in the transition region) with one-foot anchored in the umbra. We assume that it is this loop that is the magnetic channel. This indicates at a possibility of wave penetration into the flare energy release region. The loop foot polarization increase from the sunspot testifies to an increase in the gyro-synchrotron emission due to a heating by the travelling agent. We assume that this agent is slow ~ 3 -min period magnetoacoustic waves that are generated in the sunspot and propagate along the magnetic loop. In the corona, the flare also showed a formation of new loop structures. We discovered a magnetic channel that coincides with the flare radio loop. The flare occurred below the magnetic channel by height. In the flare region, before the flare, there existed strong twisted magnetic loops showing the existence of strong electric currents and stored free energy. We assume that during the flare start, the electric currents were filamented into the current sheets as described by Gordovskyy et al. (2014), and thus ready for an effective reconnection. We found that, before the flare maximum, a continuous increase in the power of 3-min sunspot oscillations is observed both in the transition region and in the corona. In the corona, this increase is related to the lengthening of wave propagation distance, reaching its maximum after the flare main phase. A rope of thin magnetic loops is formed, along which 3-min coronal waves propagate into the flare region. Simultaneously, as the wave trains move toward the loop top, a growth in their velocity is observed. Due to the existence of centrifugal forces, a portion of the longitudinal wave energy may convert into transverse waves during the wave propagation in the curvilinear magnetic fields as described by Zaitsev and Stepanov (1989). Observations in the radio range, where we see an emergence of the radio loop transverse oscillations at the beginning of the flare, corroborate this. The transverse oscillation emergence is related to the energy increase in the 3-min longitudinal waves propagating from the sunspot along the flare loop. We assume that the transverse waves emerging in the magnetic channel may lead to magnetic reconnections of the thin current sheets in the underlying twisted loops, and initiate the flare. The additional energy release process may lead to the formation of the flat stage on the flare time profile in soft X-ray. When the wave feed ends, a decrease in the X-ray radiation starts. Simultaneously, the flare loop temperature decreases, as seen from the flare loop disappearance in the

94 Å high-temperature channel (6.3 MK) images, and their appearance in the colder 171 Å coronal channel (1 MK). The formation of the flat flare stage in soft X-rays was accompanied by the temperature variations, which indicates the periodic reconnections caused by wave processes.

5. Conclusions

We analyzed the relation between the sunspot umbra oscillations and the occurrence of a small flare in the adjacent region. The observational data at the level of the transition region (NoRH, radio) and of the corona (SDO/AIA, ultraviolet) were used. We performed the analysis by using time-distance plots and pixel wavelet filtration (PWF method). The obtained results can be summarized as follows:

- C1.5 flare profiles in active group NOAA 11494 showed three peaks in the radio and in the ultraviolet radiation spaced by time and by the emission generation height. The flare started with type III bursts at about 400 MHz which was followed by a noise storm in the 200-300 MHz range. In soft X-rays (6-12 keV), a flat stage with an ~ 3 -min period flux modulation is observed.
- Correlation curves (17 GHz) show sunspot radio-frequency oscillations in sunspot with an ~ 3 -min period. The pulsations have a train character with a 12-20-min period. Each train drifted in periods in the range of 2-4 minutes. The drift value decreases toward the flare onset. This indicates the formation of a spatially magnetic rope (channel), along which slow magnetoacoustic waves start to propagate.
- The radio curves show a monotonous, linear increase in the oscillation train power two hours prior to the flare. The power maximum is observed 30 minutes before the flare. We assume the oscillation power increase due to a local efflux of subphotospheric impulses. This increase may be associated with the flare emergence, provided their participation in the forced reconnection initiation process. In this case, waves may appear as a flare process trigger.
- The source of radio pulsations represents a loop source, whose one footpoint is anchored in the umbra. Waves propagate from the sunspot toward the flare region. For the first time, we found the observational data for the process of transformation of longitudinal low-frequency 3-min waves propagating from the sunspot into the transverse high-frequency loop oscillations with an ~ 30 -40 sec period.
- In the corona region (SDO/AIA, 171 Å), the source of the UV 3-min oscillations coincides with the radio loop. Its shape looks like an arrow localized in the umbra and directed toward the future flare. Further, the arrow extends, and a fine-structure rope of magnetic loops (waveguides) forms. This rope connects the sunspot with the flare region.
- The propagation length of 3-min waves starts to monotonically increase and proceeds beyond the umbra boundary ~ 30 minutes prior to the flare onset. This coincides with the oscillation peak on the 17 GHz correlation curve and with the evolution of loops in 171 Å. The wave velocity along the loop grows from 36.2 km s⁻¹ in the sunspot to 84.6 km s⁻¹ near the loop top.
- A heating of the flare loops looks to be caused by the transversally oscillating magnetic waveguide periodically triggering the magnetic reconnections in the underlying twisted loops. As the 3-min wave trains extended, a reconnection region expansion occurred. During the flare the magnetic field configuration became simpler; the primary twist of loops disappeared.
- The flux profile in soft X-rays has a flat stage after the main peak. We assume that the emergence of this stage is associated with an additional energy release due to the mechanism for the forced quasi-periodic reconnections with the underlying loops initiated by the flare loop transverse oscillations.

6. Acknowledgements

This work was supported by the Russian Foundation for Basic Research under Grants 13-02-00044, 13-02-90472, 14-02-91157, Marie Curie International Research Staff Exchange Scheme Fellowship within the 7th European Community Framework Programme (PIRSES-GA-2011-295272 RadioSun project), Grant P209/12/0103 (GA ČR) and F-CHROMA European Union project 606862. JD acknowledges support from the Royal Society via the Newton International Fellowships Programme.

References

- Abramov-Maximov V. E., Gelfreikh G. B., & Shibasaki K. 2011, *Sol. Phys.*, 273, 403
- Alissandrakis, C. E. 1981, *A&A*, 100, 197
- Aulanier G., Parlat E., Demoulin P., & DeVore, C. R. 2006, *Sol. Phys.*, 238, 347
- Aulanier G., Janvier M., & Schmieder, B. 2012, *A&A*, 543, A110;
- Dudík J., Janvier M., Aulanier G., et al. 2014, *ApJ*, 784, 144
- Gary, G. A. 1989, *ApJS*, 69, 323
- Gordovskyy M., Browning P. K., Kontar E. P., & Bian N. H. 2014, *A&A*, 561, A72
- Karlický M., & Jungwirth K. 1989, *Sol. Phys.*, 124, 319
- Kotrč P., Kupryakov Yu. A., Kashapova L. K., & Bárta, M. 2013, *Central European Astrophysical Bulletin*, 37, 555
- Kupriyanova E. G., Melnikov V. F., & Shibasaki, K. 2013, *Sol. Phys.*, 284, 559
- Lemen, J. R., Title, A. M., Akin, D. J., et al. 2012, *Sol. Phys.*, 257, 17
- Liu C., Lee J., Karlický M., et al. 2009, *ApJ*, 703, 757
- Nakariakov V. M., Foullon C., Verwichte E., & Young N. P. 2006, *A&A*, 452, 343
- Norman C. A., & Smith R. A. 1978, *A&A*, 68, 145
- Odstrčil D., & Karlický, M. 1997, *A&A*, 326, 1252
- Schwer K., Lilly R. B., Thompson B. J., & Brewer D. A. 2002, *AGU Fall Meeting Abstracts*, SH21C-01
- Shibasaki K. 2001, *ApJ*, 550, 1113
- Sych R. A. & Nakariakov V. M. 2008, *Sol. Phys.*, 248, 395
- Sych R., Nakariakov V. M., Karlický M., & Anfinogentov, S. 2009, *A&A*, 505, 791
- Sych R., Zaqarashvili T.V., & Nakariakov V.M. et al. 2012, *A&A*, 539, A23
- Title A. M., Hoeksema J. T., Schrijver C. J., & The AIA Team 2006, *36th COSPAR Scientific Assembly*, 2600
- Zaitsev V. V., & Stepanov A. V. 1989, *Soviet Astronomy Letters*, 15, 66
- Zuccarello F., Romano P., Fárník F., et al. 2009, *A&A*, 493, 629